EXPERIMENTAL DIFFICULTIES IN MEASURING SEPARATING BOUNDARY LAYERS WITH THE LDV TECHNIQUE

Francesca Satta, Daniele Simoni, Marina Ubaldi, Pietro Zunino

Dipartimento di Macchine, Sistemi Energetici e Trasporti
Università di Genova
Genova, Italy

ABSTRACT

Laser Doppler Velocimetry is a powerful instrumentation for experimental investigations of separating boundary layers. In recent experiments performed by the authors on turbulent boundary layer separation control some practical problems have been encountered:

- wall light reflections that prevent measuring in the boundary layer linear sublayer;
- statistical errors in separating flow regions where large flow structures are present;
- statistical bias in the probability density function estimate, due to the different probability of low and high velocity particles to pass through the probe volume.

Possible solutions of these problems are suggested and evaluated in the present paper.

INTRODUCTION

Laser Doppler Velocimetry has proved to be a powerful technique for accurate turbulent boundary layer investigations, particularly when separation occurs and other techniques, such as hot-wire or hot-film anemometry, cannot recognize reverse flows. However, when measuring separating turbulent boundary layers even with the LDV technique, some difficulties of different nature may be encountered. Three kinds of problems are analysed in the present paper.

The first problem concerns the wall light reflections. The reduction of reflections in order to measure as close as possible to the wall constitutes a starting point for detailed and accurate measurements. In the present work, different solutions are considered for this purpose.

A second problem may come out when the flow is characterized by large integral time scales. In this case, in fact, a reduction of the number of independent samples occurs, because the integral time scale of the flow becomes much larger than the sampling period, with the consequence of collecting more samples inside the same eddy and hence increasing the statistical error. This issue is addressed in the present work and the reduction of independent samples associated to the increase of the integral time scale for separating boundary layers has been evaluated.

Finally when analysing intermittent reverse flows, the probability density function (pdf) of the particles velocity may be not completely representative of pdf of the flow velocity, due to the different probability that low and high velocity particles pass through the probe volume. A new procedure to evaluate flow velocity pdf from LDV data is proposed in the paper.

NOMENCLATURE

C_f	skin friction coefficient $= \frac{\tau_w}{\frac{1}{2}\rho U^2}$
H_{12}	shape factor $= \frac{\delta^*}{\vartheta}$
n	number of occurrences inside the bin
N_b	bins number
p, pdf	probability density function
Re_θ	momentum thickness Reynolds number $= U_0\theta/\nu$
rms*(u')*	root mean square of the streamwise velocity fluctuations
S	power spectral density
T_i	integral time scale
tt	particle transit time
TT	mean transit time of all the particles
Tu	free-stream turbulence intensity = rms*(u')*/*U*
U	free-stream velocity
u	streamwise velocity
u_τ	wall friction velocity $= \sqrt{\tau_w/\rho}$
u^+	boundary layer inner variable $= \frac{\overline{u}}{u_\tau}$
x	axial coordinate from the test section inlet
y	distance from the wall
y^+	boundary layer inner variable $= y\frac{u_\tau}{\nu}$
δ	boundary layer thickness

δ^* displacement thickness = $\int_0^{\delta}(1-\frac{\overline{u}}{U})dy$

Δu velocity interval

θ momentum thickness = $\int_0^{\delta}\frac{\overline{u}}{U}(1-\frac{\overline{u}}{U})dy$

ν kinematic viscosity

ρ density

τ_w wall shear stress

Subscripts and superscripts

j bin index

k index of occurrences within the bin

m mean

w weighted

‘ fluctuating quantity

—— time averaged quantity

EXPERIMENTAL APPARATUS

Investigations on turbulent boundary layer separation control have been recently carried out in an open-loop blow-down wind tunnel (Fig. 1), with a test section constituted by a large-scale flat plate on which the turbulent boundary layer develops and an opposite wall with variable inclination, which feature a 2D diffuser with variable aperture angle.

Figure 1. Experimental apparatus

Measurements have been performed on the bottom flat plate, where the prescribed adverse pressure gradient has been imposed by regulating the top wall inclination. For the present work the diffuser was set at an aperture angle of 16°. The test section geometry is shown in Fig. 2.

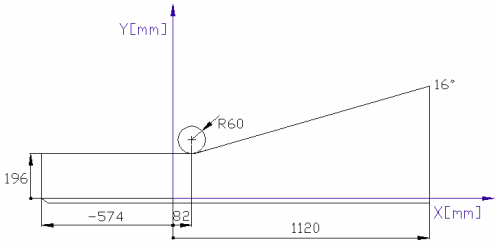

Figure 2. Test section scheme

The flat plate is 1700 mm long and 400 mm wide, its leading edge is located about 600 mm upstream of test section inlet. The inlet test section height is 196 mm. Suction is applied to the top wall boundary layer in order to avoid interactions with the lower flat plate boundary layer. Further details of the test rig can be found in a previous authors' work [1].

The boundary layer parameters at the test section inlet, typical of a turbulent boundary layer, are shown in Tab. 1.

Table 1. Boundary layer parameters at the test section inlet

δ	θ	H_{12}	Re_θ	c_f	Tu
80 mm	5.6 mm	1.24	11000	0.0032	1%

LASER DOPPLER VELOCIMETRY INSTRUMENTATION

A four beams two colours Laser Doppler Velocimeter (Dantec Fiber Flow), in backward scatter configuration, was employed for the present study. The light sources are two diode-pumped solid state lasers with a power of 200 mW each one. The two pairs of green and blue beams, employed to investigate the two velocity components, have respectively wave lengths of 532 nm and 488 nm. The frequency of one of each pair of beams was shifted of 40 MHz by a Bragg cell. The probe consists of an optical transducer head of 60 mm diameter, with a focal length of 300 mm and a beam separation of 38 mm, connected to the emitting optics and to the photomultipliers by means of optic fibres. The beam intersection angle is 7.4°. The fringe separation is 4.1 μm for the green pair of beams and 3.8 μm for the blue one. The probe volume is 0.09 mm x 0.09 mm x 1.4 mm. Flow was seeded with mineral oil droplets of 1.5 μm mean diameter. To process bursts, two Dantec Enhanced Burst Spectrum Analysers operating in coincidence mode were employed. For each measurement point, 30000 samples were collected with a maximum record length in time of 120 s.

WALL REFLECTIONS REDUCTION

Turbulent boundary layer analysis cannot leave out of consideration a careful evaluation of the near wall region characteristics. This requirement is even more critical when a separating boundary layer is studied.

Typical velocity profiles of a turbulent boundary layer subjected to strong adverse pressure gradient are shown in Fig. 3. Three different axial locations are considered. It is possible to observe a progressive reduction of the log-law region with the axial coordinate increase, due to the strong adverse pressure gradient, and the consequent reduction of the wall shear stress. Moving toward the detachment point (detected for x = 385 mm), only the viscous sublayer law is valid. Since buffer

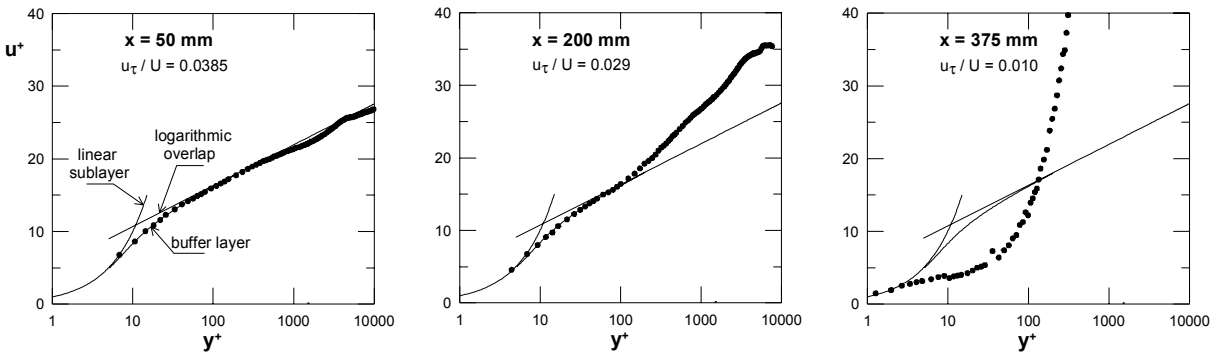

Figure 3. Wall coordinates velocity profiles

layer and logarithmic laws are not followed in separating regions, measurements in the linear sublayer are needed to allow wall shear stress evaluation. Fortunately the reduction of friction velocity determines the decrease of the values of y^+ for measuring points located at the same distances from the wall. Nevertheless, the reduction of light reflections, in order to measure as close as possible to the wall, remains the prerequisite for boundary layer significant measurements.

If the aluminium surface (that behaves such as a mirror surface) is not subjected to any treatment, strong wall reflections occur, as shown in Fig. 4, which determine a very poor data rate at a distance from the wall of 100 μm.

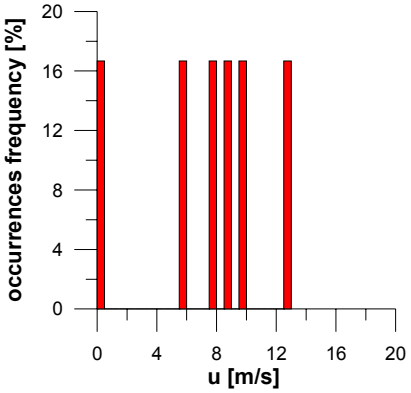

Figure 4. Occurrences frequency distribution with aluminium surface, at y = 100 μm

On the contrary, employing an orange fluorescent paint, the flat plate works as a re-emitting surface, and green and blue reflections are completely suppressed, as shown in the occurrences frequency distribution of Fig. 5, but unfortunately with this surface treatment the measuring point nearest to the wall has to be located at least at y =100 mm, in order to avoid paint burn out. This problem was finally circumvented by treating the surface with a black opaque paint that allowed to avoid light reflections (Fig. 6) up to 50 μm from the wall, without being subjected to burning out.

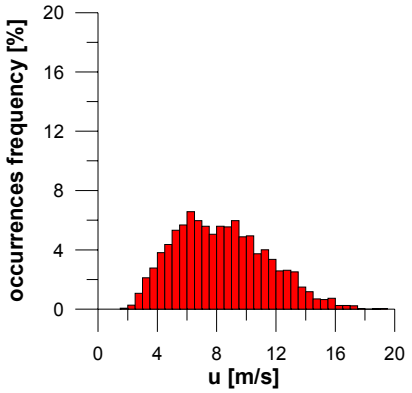

Figure 5. Occurrences frequency distribution with orange fluorescent paint, at y = 100 μm

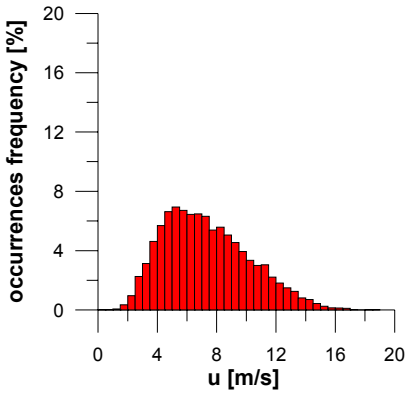

Figure 6. Occurrences frequency distribution with black opaque paint, at y = 50 μm

The velocity profiles in wall coordinates for the three different surface treatments are shown in Fig. 7. In the case of no treatment, the experimental data fail to follow the theoretical laws, because of the wall light reflections. In the other two cases the points follow precisely the wall laws. With the black opaque paint the first point could be collected in the linear sublayer, demonstrating that this very simple surface treatment is suitable for near wall measurements.

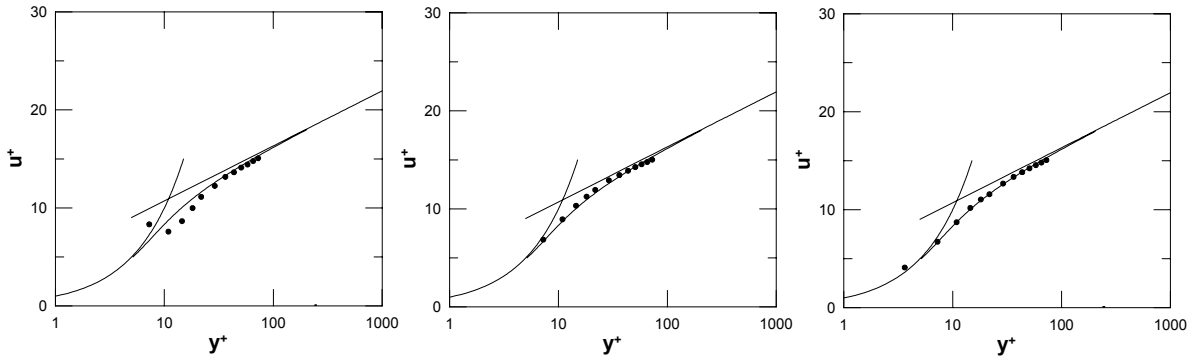

Figure 7. Wall coordinates velocity profiles at x = 0 mm obtained with (from left to right): aluminium, orange fluorescent painted, and black opaque painted surfaces

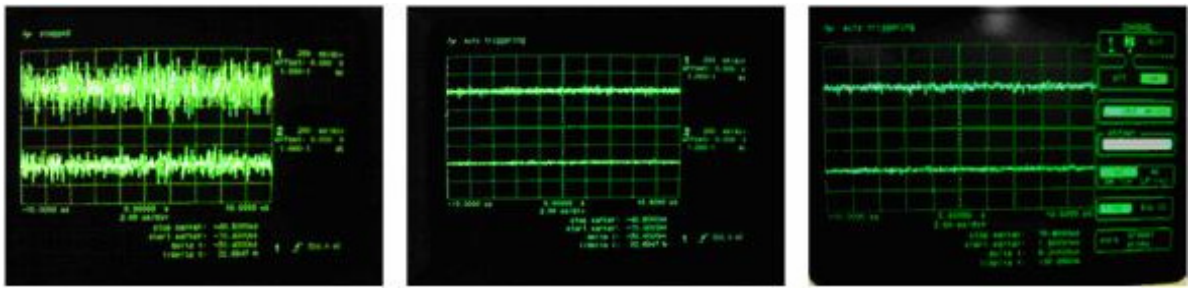

Figure 8. Photomultipliers output at the zero position obtained with (from left to right): aluminium, orange fluorescent painted, and black opaque painted surfaces

What shown before about the wall reflections is confirmed by observing the photomultipliers outputs when the probe volume is located on the surface at y=0 (Fig. 8). In fact, in the cases of fluorescent and black opaque paints the signal to noise ratio is much lower than that obtained with the aluminium surface.

STATISTICAL ERRORS REDUCTION

The second problem encountered during the LDV measurements in the separating turbulent boundary layer concerns the statistical error that may occur in a separating flow.

An accurate statistical analysis of the data requires statistically independent collected samples. For this reason, once the number of samples is fixed, the sampling period should not be smaller than the integral time scale of the flow [2, 3].

The integral time scale of the flow can be evaluated from the power spectral density of the velocity [4]

$$T_i = \frac{S_{f\to 0}}{2\overline{u'^2}} \qquad (1)$$

To determine the power spectrum, a high data rate of LDV measurements is required in order to reconstruct a pseudo-time history of the velocity [6]. Therefore, measurements were carried out at the maximum data rate obtainable. Due to the discontinuous and random transit of particles the time history is a discrete and non equi-spaced time series. The power spectral density therefore has been evaluated using a sample and hold technique with multisample interpolation. This technique produces a filtering noise which acts like a low pass filter [6], which attenuates the spectrum at frequencies larger than $f_s/2\pi$. However, it is expected that the spectral density is unaffected by bias when frequency tends to zero.

To validate the procedure, the integral time scale evaluated from LDV measurements at the test section inlet has been compared with that obtained by means of a hot-wire anemometer (Fig. 9). A good agreement between the two distributions comes out from the comparison.

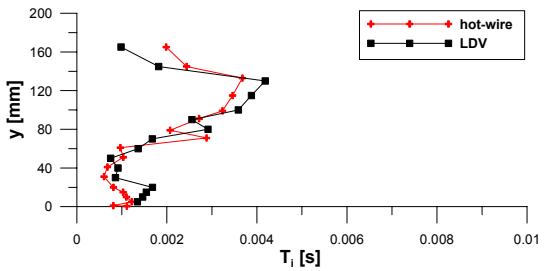

Figure 9. Comparison of integral time scales obtained with hot-wire anemometer and LDV

Once confirmed the applicability of the procedure, flow integral time scales have been calculated for all the axial traverses. Results obtained are shown in the contour plot of Fig. 10.

In the region of attached boundary layer the integral time scale T_i assumes nearly constant low values, which are of the order of 1 ms. Only in the external region, especially nearby the test section inlet, the presence of larger freestream structures

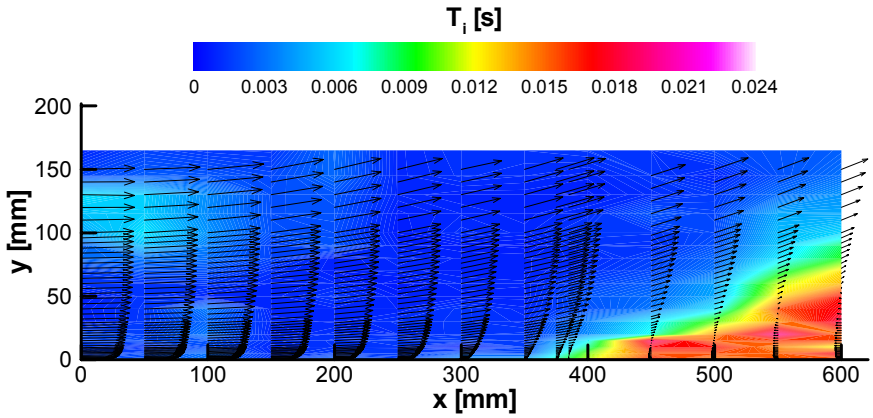

Figure 10. Flow integral time scales contour plot

determines larger values for T_i. Before the detachment line and in detached region (detachment point detected at the wall at x=385 mm) the integral time scale increases significantly, due to the formation of large scale flow structures, as postulated by Simpson and Chew [7].

As discussed above, where the integral time scale is larger than the sampling period, the number of independent samples decreases, because more samples are collected inside the same eddy. For this reason a measurement campaign with low data rate has been carried out in order to reduce the statistical error.

According to George [3], the statistical error of the mean velocity when the realizations may not be independent can be evaluated by

$$e^2 = \frac{(1+2\,f_s\,T_i)}{N}(\mathrm{rms}(u')/\overline{u})^2 \qquad (2)$$

where f_s is the mean data rate and N is the total number of realizations.

Therefore, when the integral time scale increases, the data rate should be reduced in order to decrease the statistical error. In the first measurement campaign, carried out at high data rate (ranging from 500 to 3000 Hz) in order to be able to evaluate the integral time scales of the flow, a large effect of independent samples reduction occurred downstream of the detachment point, as shown in Fig. 11, where the distribution of the term $(1+2\,f_s\,T_i)$ is represented.

Decreasing the data rate values (f_s = 100-500 Hz), the independent samples reduction largely decreases even in the separated region, as shown in Fig. 12.

The distributions of the statistical error of the mean velocity are reported in Fig. 13 for the two measuring campaigns (high and low data rate cases). The errors are lower for low data rate. However, they are not very high for both the cases.

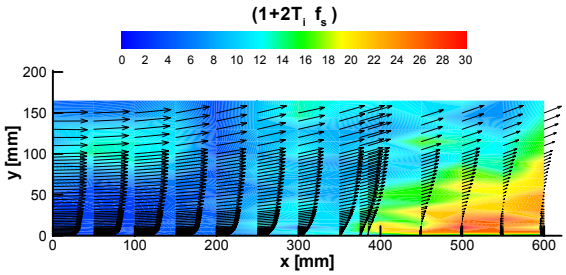

Figure 11. Reduction of independent samples with high data rate (f_s = 500 - 3000 Hz)

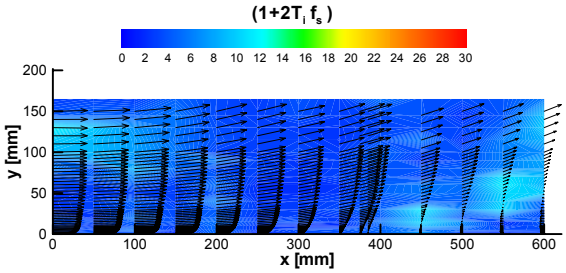

Figure 12. Reduction of independent samples with low data rate (f_s = 100 - 500 Hz)

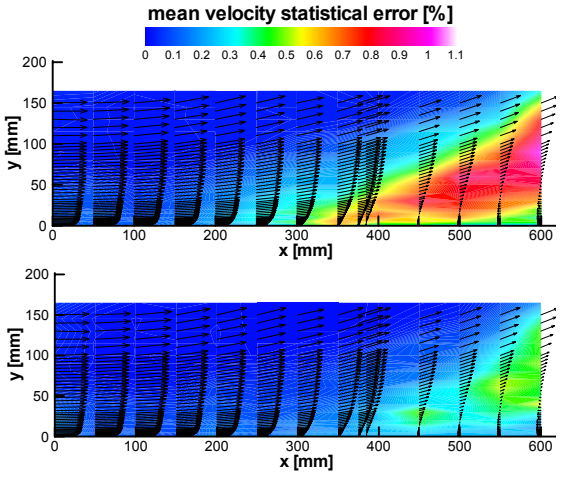

Figure 13. Mean velocity statistical error with high (top) and low (bottom) data rates

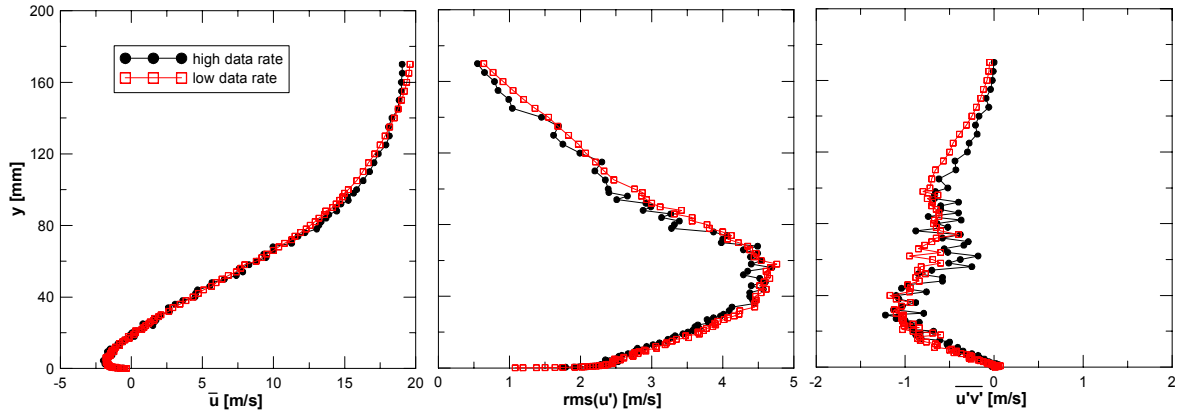

Figure 14. Comparison of mean velocity, root mean square of the velocity fluctuations and Reynolds shear stress obtained with high and low data rates, at x = 500 mm

Larger errors affect the second order velocity moments, as demonstrated by the oscillations in the rms and Reynolds stress distributions at x=500 mm for the case with high data rate, as it can be observed in Fig. 14. That confirms the necessity of operating with an appropriate data rate in order to reduce the statistical errors, especially for second order velocity moments.

PROBABILITY DENSITY FUNCTION OF THE FLOW VELOCITY

In the separating turbulent boundary layer, the probability density function estimate from LDV data processing presents two peaks, for positive and negative velocity values (Fig. 15).

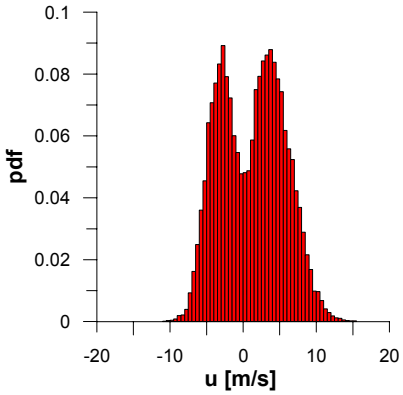

Figure 15. Probability density function estimate obtained in the separated zone

This distribution may suggest that the flow time structure is characterized by switching between two high probability states with positive and negative velocities and that low velocity values are less probable. Indeed the distribution of Fig. 15 is the correct pdf estimate of the velocity of the seeding particles that cross the measuring volume, but may not be the correct pdf estimate of the flow velocity. Probability density function estimated by Simpson [8] in a separating boundary layer displays a single peak distribution. Simpson claimed that his pdf should not be affected by statistical bias, since his burst processing technique was based on "the sampling spectrum analysis", that makes use of an analogue spectrum analyser and a sample and hold circuit for data sampling.

Looking at the particles transit time as a function of the velocity for the same measuring point (Fig. 16) one can see that for low velocities the transit time is much larger than the mean value. Therefore, it is expected that particles with lower velocities have lower probability to pass through the probe volume, according to McGlaughlin and Tiederman analysis [9].

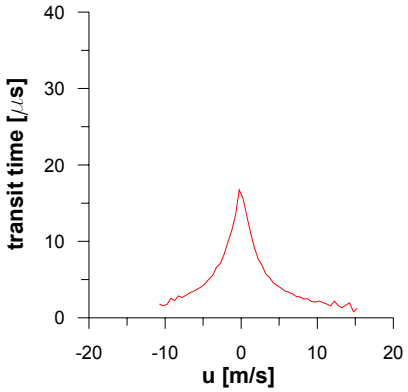

Figure 16. Transit time distribution for the measuring point of Fig. 15

Usually the pdf estimate for a sampled function is evaluated by the following relationship:

$$p_j = \frac{n_j}{\Delta u \sum_{j=1}^{N_b} n_j} \qquad (3)$$

where p_j in case of LDV measurements represents the "particle velocity probability".

In the following it is proposed a procedure that extend the transit-time-weighted averaging technique of McGlaughlin and Tiederman [9] to the evaluation of the probability density function of the flow velocity.

The transit-time-weighted velocity is given by

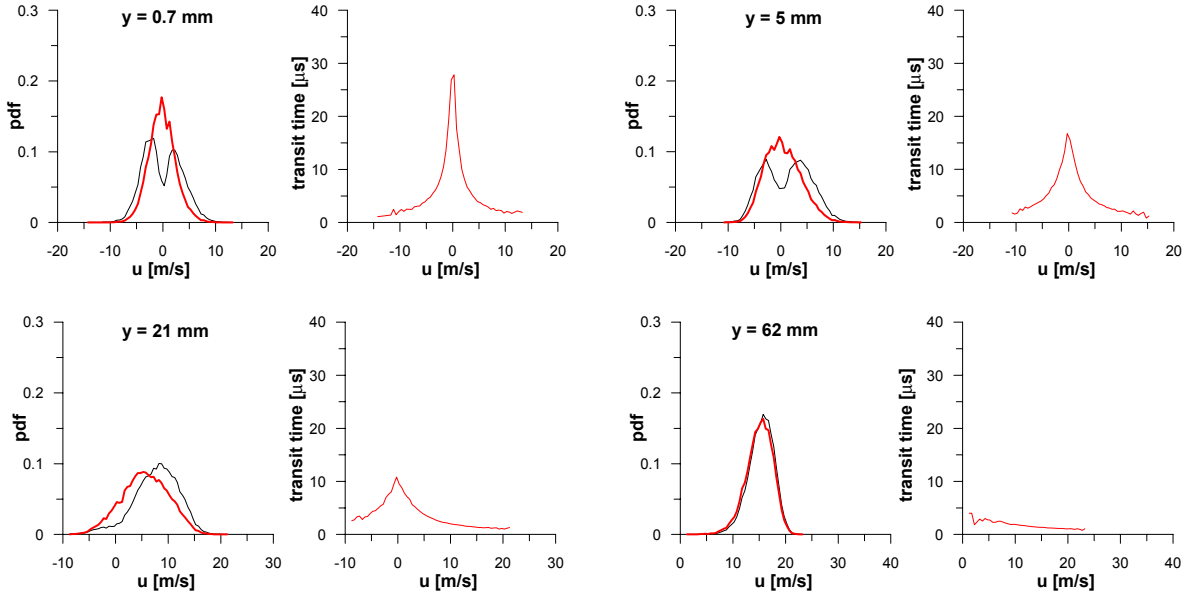

Figure 17. Pdf estimates comparison (black curves: particle velocity probability eq.(3); red curves: flow velocity probability eq. (5)) and transit time distributions for different points at x = 385 mm

$$u_w = \frac{\sum_{i=1}^{N} u_i \, tt_i}{\sum_{i=1}^{N} tt_i} \qquad (4)$$

In order to determine the pdf estimate of the flow velocity, it is necessary to take into account the lower occurrences of low velocity particles in the probe volume, and for this reason it is here proposed to weight each particle occurrence with its transit time:

$$(p_w)_j = \frac{\sum_{k=1}^{n_j} (tt_{k,j} / TT_m)}{\Delta u \sum_{j=1}^{N_b} \sum_{k=1}^{n_j} (tt_{k,j} / TT_m)} = \frac{\sum_{k=1}^{n_j} tt_{k,j}}{\Delta u \sum_{j=1}^{N_b} \sum_{k=1}^{n_j} (tt_{k,j})} \qquad (5)$$

In Fig. 17, the usual pdf estimates (black curves) are compared with those obtained weighting the occurrences with the particle transit time (red curves), for some points of the traverse at x = 385 mm. It is possible to observe how, when peaks in the transit time distributions are present, the pdf estimate is largely corrected by the transit time, and particularly, when two peaks are present in the pdf of the particle velocity, they disappear in the corrected one, thanks to the higher weight associated to the low velocity particles. The pdf distribution obtained weighting the occurrences with the transit time, therefore, suggests that the two peaks are not representative of the flow, and the corrected pdf presents a nearly Gaussian distribution, or in other words the most probable value in a separating boundary layer is the zero velocity. This is in agreement with the pdf evaluated by Simpson [8].

To verify if the procedure proposed is appropriate to obtain the pdf of the flow, the mean velocity distribution obtained from the corrected pdf estimate has been compared with the transit-time-weighted velocity and with the simple arithmetic average u_m.

Since the mean velocity u_m can be obtained integrating the product $p(u) \cdot u$,

$$u_m = \int_{-\infty}^{\infty} p(u) u \, du \cong \sum_{j=1}^{N_b} p_j u_j \Delta u = \frac{\sum_{j=1}^{N_b} n_j u_j}{\sum_{j=1}^{N_b} n_j} \qquad (6)$$

similarly the transit-time-weighted velocity u_w can be obtained employing the following equation:

$$\sum_{j=1}^{N_b} (p_w)_j u_j \Delta u = \frac{\sum_{j=1}^{N_b} u_j \sum_{k=1}^{n_j} tt_{k,j}}{\sum_{j=1}^{N_b} \sum_{k=1}^{n_j} (tt_{k,j})} \cong u_w \qquad (7)$$

In Fig. 18 the comparison of boundary layer mean velocity profiles at the detachment point obtained from the three different averaging procedures (applying equations 4, 6 and 7) is shown.

These velocity distributions demonstrate that the mean velocity profile obtained from the corrected pdf estimate is consistent with the transit-time-weighted velocity. Therefore the pdf estimate obtained weighting the occurrences with the particle transit-time is representative of the probability density distribution of the flow velocity.

CONCLUSIONS

Detailed experiments on separating boundary layers, even if carried out with an adequate

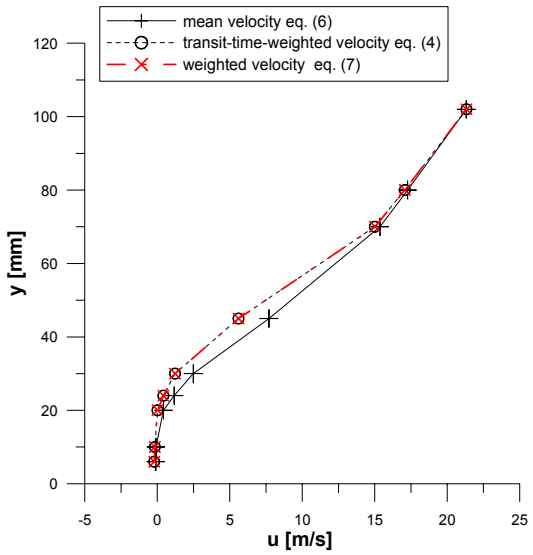

Figure 18. Comparison of mean velocity profiles obtained with different procedures at x = 385 mm

measuring technique such as LDV, may present difficulties.

The first difficulty consists in the possibility of measuring as near as possible to the wall, avoiding surface reflections. For this purpose, the surface where experiments were carried out has been treated with different paints. The black opaque paint resulted to be the most suitable for near wall measurements. With this wall treatment measures up to a distance from the wall of 50 μm (approximately half of the probe volume diameter) were allowed.

Another problem that may occur particularly in separating flow regions concerns the presence of large flow structures that reduce the number of independent samples. It was found that, in order to obtain measurements with low statistical errors, the knowledge of the flow integral scale is useful. This gives an indication of the appropriate mean data rate to be adopted in order to reduce the statistical errors.

Moreover, in regions with intermittent reverse flow the statistical bias due to the different probability of passing through the probe volume of particles with different velocities is significant and affects the probability density function estimate. It was found that particle velocity probability is not representative of flow velocity probability. A procedure to obtain the flow velocity probability density function has been suggested in the paper, which is consistent with the unbiased transit-time-weighted velocity.

REFERENCES

[1] Canepa, E., Lengani, D., Satta, F., Spano, E., Ubaldi, M., Zunino, P., 2006, "Boundary Layer Separation Control on a Flat Plate With Adverse Pressure Gradients Using Vortex Generators", ASME Paper n° GT2006-90809.

[2] George, W.K., 1978, ''Processing of Random Signals'', Proceedings of the Dynamic Flow Conference, pp. 757-800.

[3] George, W.K., 1988, "Quantitative Measurements with the Burst-Mode Laser Doppler Anemometer", *Experimental Thermal and Fluid Science*, vol. 1, pp. 29-40

[4] Cebeci, T., Smith A.M.O., 1974, Analysis of Turbulent Boundary Layers, Academic Press, New York.

[5] Campora, U., Pittaluga, F., Ubaldi, M., Zunino, P., 2002, "A Detailed Investigation of the Transitional Boundary Layer on the Suction Side of a Turbine Blade", XVth Bi-Annual Symposium on Measuring Techniques in Transonic and Supersonic Flows in Cascades and Turbomachines, Firenze.

[6] Adrian, R.J., Yao, C.S., 1987, "Power Spectra of Fluid Velocities Measured by Laser Doppler velocimetry", *Experiments in Fluids*, vol. 5, pp. 17-28.

[7] Simpson, R.L., Chew, Y.T., 1981, "The Structure of a Separating Turbulent Boundary Layer. Part 1: Mean Flow and Reynolds Stresses", *Journal of Fluid Mechanics*, vol. 113, pp. 23-51.

[8] Simpson, R.L., 1976, "Interpreting Laser and Hot-Film Anemometer Signals in a Separating Boundary Layer", *AIAA Journal*, vol. 14, n°1, pp. 124-126.

[9] McGlaughlin, D.K., Tiederman, W.G., 1973, "Biasing Correction for Individual Realization Laser Anemometer Measurement in Turbulent Flows", *Physics of Fluids*, vol. 16, n° 12, pp. 2082-2088.